

Article

# Palladium Supported on Carbon Nanotubes as a High-Performance Catalyst for the Dehydrogenation of Dodecahydro-N-ethylcarbazole

Mengyan Zhu <sup>1,2</sup>, Lixin Xu <sup>1,2</sup>, Lin Du <sup>3</sup>, Yue An <sup>4</sup> and Chao Wan <sup>1,2,4,\*</sup> 

<sup>1</sup> Hexian Chemical Industrial Development Institute, School of Chemistry and Chemical Engineering, Anhui University of Technology, Ma'anshan 243002, China; AHUT.zhummy@outlook.com (M.Z.); lxxu@hotmail.com (L.X.)

<sup>2</sup> Ahut Chemical Science & Technology Co., Ltd., Ma'anshan 243002, China

<sup>3</sup> Anhui Haide Chemical Technology Co., Ltd., Ma'anshan 243002, China; AHUT.dulin@outlook.com

<sup>4</sup> College of Chemical and Biological Engineering, Zhejiang University, Hangzhou 310027, China; zju.anyue@hotmail.com

\* Correspondence: wanchao1219@hotmail.com; Tel.: +86-555-231-1807

Received: 20 November 2018; Accepted: 6 December 2018; Published: 8 December 2018



**Abstract:** Hydrogen storage in the form of liquid organic hydrides, especially N-ethylcarbazole, has been regarded as a promising technology for substituting traditional fossil fuels owing to its unique merits such as high volumetric, gravimetric hydrogen capacity and safe transportation. However, unsatisfactory dehydrogenation has impeded the widespread application of N-ethylcarbazole as ideal hydrogen storage materials in hydrogen energy. Therefore, designing catalysts with outstanding performance is of importance to address this problem. In the present work, for the first time, we have synthesized Pd nanoparticles immobilized on carbon nanotubes (Pd/CNTs) with different palladium loading through an alcohol reduction technique. A series of characterization technologies, such as X-ray diffraction (XRD), inductively coupled plasma-atomic emission spectrometer (ICP-AES), X-ray photoelectron spectroscopy (XPS) and transmission electron spectroscopy (TEM) were adopted to systematically explore the structure, composition, surface properties and morphology of the catalysts. The results reveal that the Pd NPs with a mean diameter of  $2.6 \pm 0.6$  nm could be dispersed uniformly on the surface of CNTs. Furthermore, Pd/CNTs with different Pd contents were applied in the hydrogen release of dodecahydro-N-ethylcarbazole. Among all of the catalysts tested, 3.0 wt% Pd/CNTs exhibited excellent catalytic performance with the conversion of 99.6% producing 5.8 wt% hydrogen at 533 K, low activation energy of  $43.8 \pm 0.2$  kJ/mol and a high recycling stability (>96.4% conversion at 5th reuse).

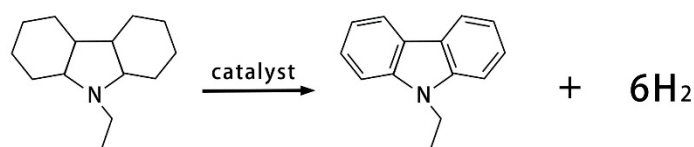
**Keywords:** palladium catalysts; CNTs; dodecahydro-N-ethylcarbazole; dehydrogenation; hydrogen storage

## 1. Introduction

Among numerous alternative energy, hydrogen has been deemed as one of the most important and ideal energy sources owing to its distinct merits, such as a high calorific value, non-toxic environmentally, sustainable and cost-effective [1–4]. As is known, a complete energy system that utilizes hydrogen as an energy source is composed of producing, storing, transporting and utilizing hydrogen. However, it is difficult for hydrogen to be stored and transported owing to its low density [5,6]. Therefore, the technology of hydrogen storage has been regarded as one of the bottlenecks for promoting the large-scale application of the hydrogen energy [5–8]. To search for new hydrogen storage technology satisfying the U.S. Department of Energy (DOE) requirements with

minimum gravimetric of 5.5 wt% and volumetric capacity of 40 g L<sup>-1</sup> remains a challenging issue for the large-scale application of hydrogen.

Among various hydrogen storage materials, such as formic acid, cyclohexane, and ammonia borane, [9–12] organic liquid hydrides have emerged as a preferred approach in existing vehicle hydrogen storage systems for its virtues like high H<sub>2</sub> storage density and safe transportation [12–14]. Especially, reversible hydrogen storage and release can be catalytically achieved under relatively moderate conditions [15,16]. Currently, hydrogenation reactions have been extensively studied in the previously reported literature [17–19]. Compared with the traditional organic liquid hydrides, the substitution of a heteroatom in heterocyclic aromatic molecules, such as in N-ethylcarbazole, can decrease the endothermicity of the reaction and bring down the dehydrogenation temperature [20,21]. Therefore, N-ethylcarbazole, with a gravimetric density of 5.8 wt.%, has been identified as the most prospective candidate for hydrogen storage (Scheme 1). Although there are many studies about the dehydrogenation reaction from calculations and experiments [20–28], the dehydrogenation reaction is still the key to limit its large-scale application, especially, the development of dehydrogenation catalysts with outstanding activity and stability is the hotspot of current research.



**Scheme 1.** Dehydrogenation pathway for dodecahydro-N-ethylcarbazole.

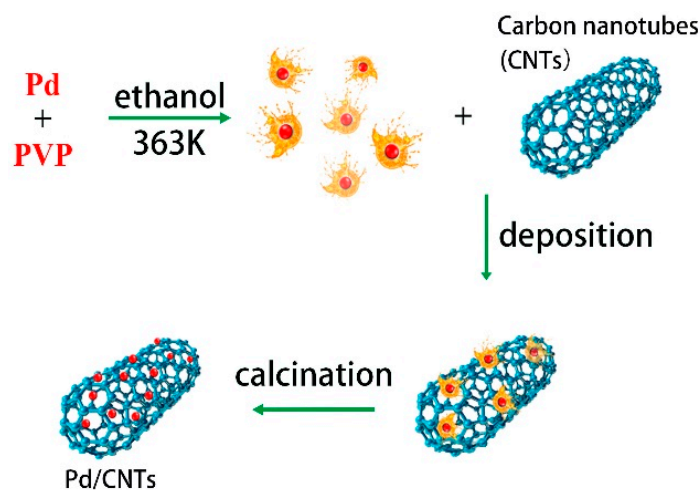
A large number of dehydrogenation catalysts have been extensively investigated, including homogeneous catalysts and the heterogeneous catalysts [29–35]. For the homogeneous catalysts, Wang et al. firstly reported the synthesis of homogeneous Ir-complex catalysts and explored its performance for the hydrogen release of dodecahydro-N-ethylcarbazole at 473 K but the dehydrogenation results were unsatisfactory [34]. However, the heterogeneous catalysts exhibited a notable advantage over homogeneous ones with respect to catalytic activity. For the heterogeneous catalysts, the supporting materials and NPs (Nanoparticles) are the two key factors influencing the catalytic performance. Yang et al. [36] have studied the dehydrogenation activity of perhydro-N-ethylcarbazole over a series of noble metal catalysts and the kinetics of dehydrogenation of dodecahydro-N-ethylcarbazole over a 5 wt% Pd/Al<sub>2</sub>O<sub>3</sub> catalyst. The results revealed that the order is Pd > Pt > Ru > Rh according to the initial catalytic activity of the investigated noble metal catalysts in the dehydrogenation process and the rate-limiting step of the entire reaction process is the transformation from tetrahydro-N-ethylcarbazole to N-ethylcarbazole. Furthermore, Kustov et al. [37] confirmed that the catalytic activity of the catalysts can be improved under microwave activation. Although Pd based catalysts supported several supports, such as alumina, silica, TiO<sub>2</sub>, MoO<sub>3</sub> and carbon [29–33,35–38], have been systematically investigated for producing hydrogen from perhydro-N-ethylcarbazole, there are no reports about CNTs as the supporting material in the hydrogen release from perhydro-N-ethylcarbazole.

In recent years, CNTs, as a one-dimensional nanomaterial, have received considerable attention as a catalyst support material due to their high specific surface area, superior electrical conductivity and outstanding chemical and thermal stability [39,40]. In addition, CNTs can endow beneficial interactions between support and metal NPs, thus improving the catalytic activity. As is well known, the synthesis method for Pd NPs, such as doping or through a supramolecular strategy, an alcohol reduction method, is another key factor for improving the dehydrogenation performance of the catalysts [35,41–44]. Fang et al. [42] have successfully synthesized Pd/rGO using ethylene glycol as a reductant for the hydrogen production of dodecahydro-N-ethylcarbazole. Constructing Pd NP catalysts using an alcohol reduction method for the dehydrogenation of dodecahydro-N-ethylcarbazole has rarely been reported.

Herein, in this work, for the first time, we have utilized an alcohol reduction method to construct CNT-supported Pd NPs (Pd/CNTs) as the catalyst for hydrogen generation from dodecahydro-N-ethylcarbazole. The catalyst has been characterized by many characterization methods, such as XRD, ICP-AES, XPS and TEM to investigate the structure, composition, surface properties and morphology of the catalysts. The dehydrogenation process of dodecahydro-N-ethylcarbazole over Pd/CNTs catalyst is also discussed.

## 2. Results and Discussion

The Pd/CNTs with different Pd contents were fabricated via an alcohol reduction route, as schematically shown in Scheme 2 [45,46]. Typically, PVP (Poly (N-vinyl-2-pyrrolidone))-Pd NPs were obtained by refluxing a solution containing  $\text{H}_2\text{PdCl}_4$ , ethanol,  $\text{H}_2\text{O}$  and PVP at 363 K for 3 h. Subsequently, the as-synthesized PVP-Pd NPs were put in the CNTs solution under magnetic stirring for 24 h. Then, the above-mentioned solution was evaporated, the catalyst was dried and calcined. The obtained products were denoted the X wt% Pd/CNTs catalysts.



**Scheme 2.** A fabrication diagram for the preparation of Pd/CNTs.

Powder X-ray diffraction (XRD) patterns were collected to explore the phase and crystal structure of the acid-treated CNTs, Pd/CNTs with different Pd contents. As shown in Figure 1, a similar XRD pattern was observed for all of the samples. All of the samples showed three obvious peaks at  $25.9^\circ$ ,  $43.8^\circ$ , and  $54.2^\circ$ , which could be ascribed to the (002), (100), and (004) reflections of graphite structure, respectively. There was only the diffraction peak of the graphite structure for the Pd/CNTs with different Pd loadings. However, no distinct characteristic diffraction corresponding to Pd NPs was detected in the XRD patterns, probably owing to the fact that the Pd loading of Pd/CNTs was too low. The diffraction peak ascribed to Pd (JCPDS (Joint Committee on Powder Diffraction Standards) no. 46-1043) could be observed for Pd/CNTs with a higher loading (20 wt%) in Figure S1 (Supporting Information). The accurate composition of Pd/CNTs was measured by an inductively coupled plasma-atomic emission spectrometer (ICP-AES), which is close to their designed content (Table S1, Supporting Information).

X-ray photoelectron spectroscopy (XPS) was performed to investigate the surface state of 3.0 wt% Pd/CNTs. As seen in Figure 2, the peaks centered at 341.0 eV ( $3d^{3/2}$  state) and 335.8 eV ( $3d_{5/2}$  state), lower than that of Pd/Rgo, can be ascribed to the  $\text{Pd}^0$  species, which is consistent with the previously reported literature [39,40,42]. Furthermore, it is worth noting that the two small peaks appeared at 343.6 eV and 337.8 eV for the Pd3d spectra of 3.0 wt% Pd/CNTs can be attributed to  $\text{Pd}^{2+}$ , may relate to the sample treatment process for the XPS measurements [47]. The nitrogen adsorption-desorption isotherms and pore-size distributions for the CNTs and 3.0 wt% Pd/CNTs are displayed in Figures S2 and S3 (Supporting Information). It can be seen that the samples present similar adsorption-desorption

curves (type IV isotherms) and pore-size distributions. The BET (Brunauer–Emmett–Teller) surface areas of the CNTs and 3.0 wt% Pd/CNTs were calculated to be 137 and 94 m<sup>2</sup> g<sup>-1</sup>, respectively. Furthermore, the microstructure of 3.0 wt% Pd/CNTs was further investigated using transmission electron microscopy (TEM) measurements (Figure 3). As displayed in Figure 3, it can be observed that the Pd NPs were uniformly dispersed on the CNTs and the small average diameter of the particle size was 2.6 ± 0.6 nm, which is consistent with the previously reported results [39,40,45,46].

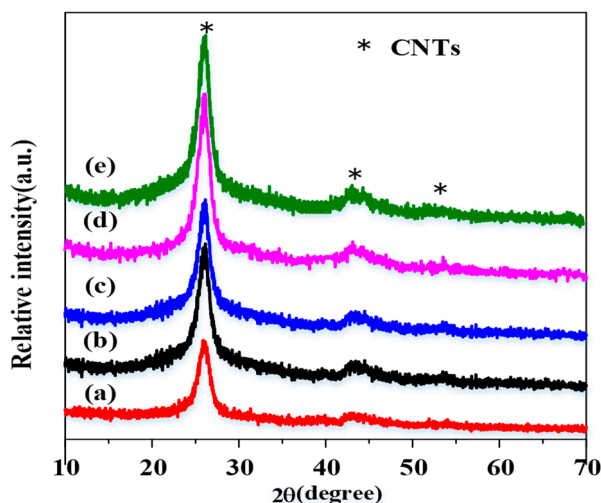


**Figure 1.** XRD patterns of (a) CNTs; Pd/CNTs with different Pd composition (b) 0.9 wt%, (c) 2.1 wt%, (d) 3.0 wt% and (e) 4.1 wt%.

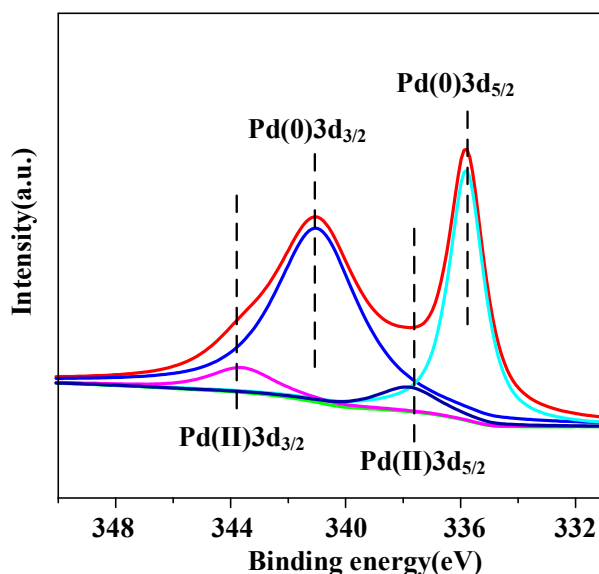


**Figure 2.** The high-resolution Pd3d peaks in the XPS spectra of 3.0 wt% Pd/CNTs.

Figure 4 shows the hydrogen release of dodecahydro-N-ethylcarbazole over Pd/CNTs with different Pd loadings in the range of 0 wt%–4.1 wt% at 513 K. The hydrogen generation rate significantly relied on the loading of Pd. As shown in Figure 4, 5.6 wt% hydrogen evolved at 90.4, 33.6, and 89.5 min in the presence of the Pd/CNTs with a Pd loading of 2.1 wt%, 3.0 wt% and 4.1 wt%, respectively. Hydrogen evolution catalyzed by 0.9 wt% Pd/CNTs only yielded 4.6 wt% hydrogen even at 97 min. However, no gas was detected for the CNT support, implying that CNTs are inactive for hydrogen production of dodecahydro-N-ethylcarbazole. Obviously, Pd/CNTs with a Pd loading of 3.0 wt% exhibited excellent catalytic activity with a conversion of 96.4%, producing 5.6 wt% H<sub>2</sub>.

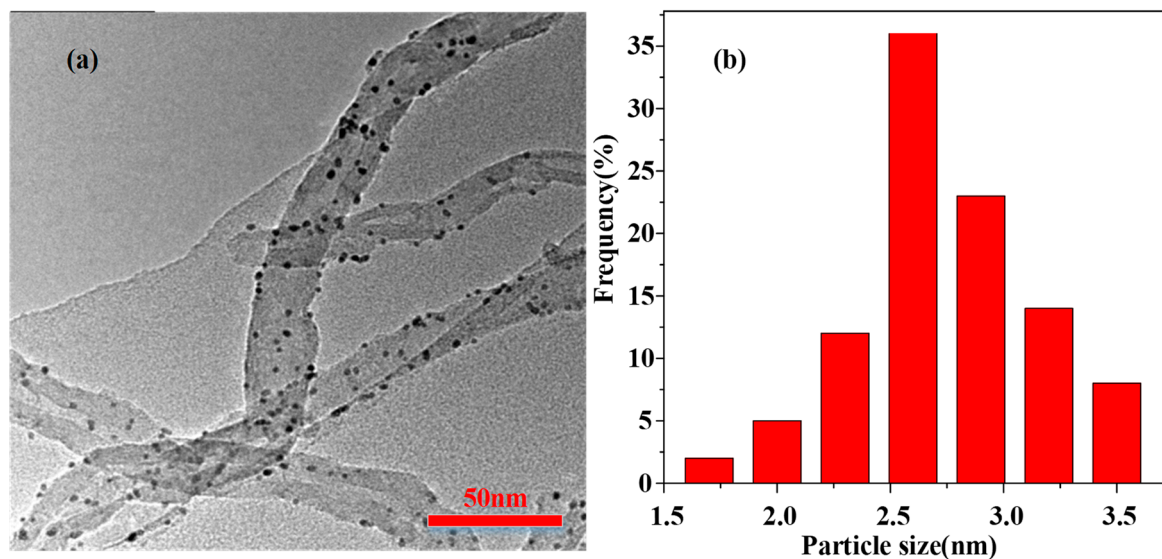


Figure 3. TEM images of (a) 3.0 wt% Pd/CNTs and (b) particle distribution.

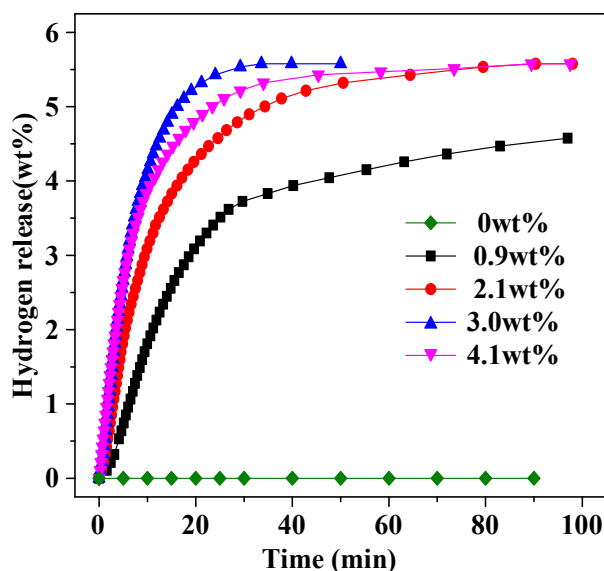


Figure 4. Hydrogen release from dodecahydro-N-ethylcarbazole catalyzed by Pd/CNTs with different Pd loadings at 513 K.

In order to explore the kinetics of the dehydrogenation of dodecahydro-N-ethylcarbazole catalyzed by 3.0 wt% Pd/CNTs, a series of experiments were carried out under varying temperatures. As displayed in Figure 5, when the temperature increased from 453 K to 533 K, hydrogen release increase from 2.7 wt% to 5.8 wt%. It is generally accepted that producing hydrogen from dodecahydro-N-ethylcarbazole is an endothermic reaction, a higher reaction temperature may be favorable for hydrogen generation from dodecahydro-N-ethylcarbazole. It can be seen in Figure 5 that the initial dehydrogenation rate and the amount of hydrogen recovery both increased with an increasing reaction temperature; the higher the reaction temperature, the higher the rate of dehydrogenation. First-order kinetics were established with the concentration of the reactant, dodecahydro-N-ethylcarbazole, measured as a function of time using 3.0 wt% Pd/CNTs catalyst [35,36,38,48,49]. The reaction rate was expressed as:

$$r = dC/dt = kC \quad (1)$$

$$\ln(C/C_0) = -kt \quad (2)$$

where  $C$  represents the concentration of dodecahydro-N-ethylcarbazole,  $C_0$  denotes the initial concentration of dodecahydro-N-ethylcarbazole.

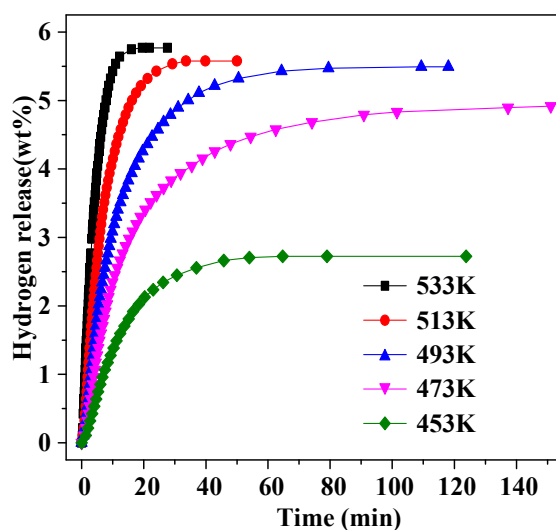


**Figure 5.** Hydrogen release of dodecahydro-N-ethylcarbazole over 3.0 wt% Pd/CNTs versus time at 453, 473, 493, 513 and 533 K.

On the basis of Figure 5 and the above formula, a linear relation of  $\ln(C/C_0)$  vs. time is observed in Figure 6a. The values of  $k$  under the different temperatures could be acquired, a smooth straight line could be observed by  $\ln k$  versus  $1/T$  plot, as demonstrated in Figure 6b, and its linear correlation coefficient was 99.6%. It is indicated that  $k$  and  $T(K)$  follow the Arrhenius equation:

$$\ln k = -E_a/(RT) + \ln k_0. \quad (3)$$

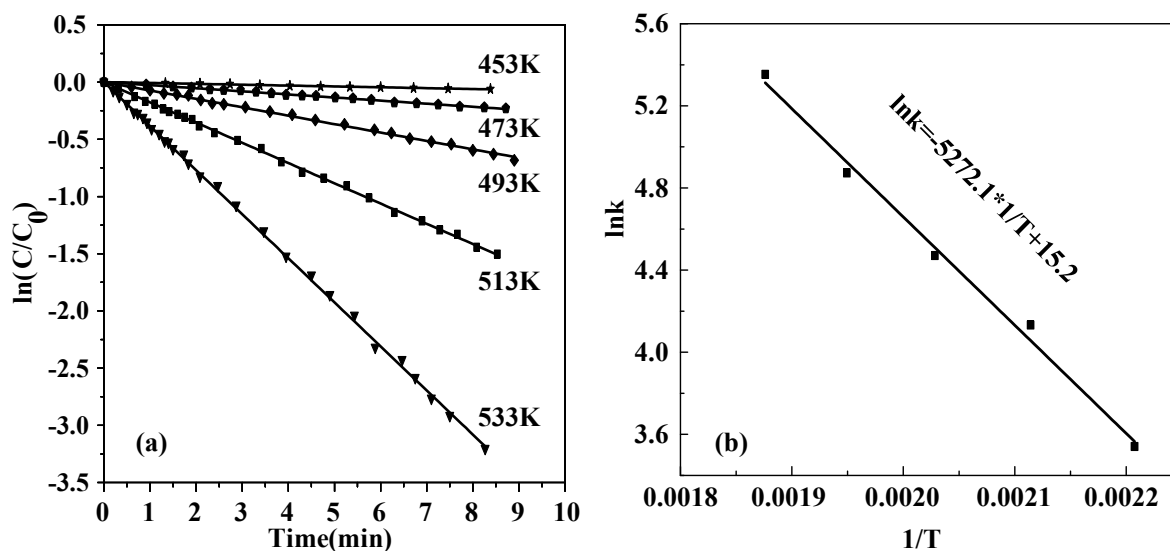


**Figure 6.** (a)  $\ln(C/C_0)$  versus time for 3.0 wt% Pd/CNTs at 453, 473, 493, 513 and 533 K; (b)  $\ln k$  versus  $1/T$  for 3.0 wt% Pd/CNTs at 453, 473, 493, 513 and 533 K.

Considering the slope of the straight line, the apparent activation energy of hydrogen production of dodecahydro-N-ethylcarbazole over 3.0 wt% Pd/CNTs was calculated to be  $43.8 \pm 0.2$  kJ/mol.

The durability of the catalyst was of significance for its practical application. Therefore, the reusability of 3.0 wt% Pd/CNTs was investigated at 533 K. As revealed in Figure 7, the catalytic

activity of 3.0 wt% Pd/CNTs shows no obvious decrease after five runs for hydrogen generation from dodecahydro-N-ethylcarbazole. The reusability tests revealed that 3.0 wt% Pd/CNTs exhibits activity in consecutive runs in the hydrogen release from dodecahydro-N-ethylcarbazole, demonstrating 96.4% conversion and 5.6 wt% H<sub>2</sub> at the fifth run.

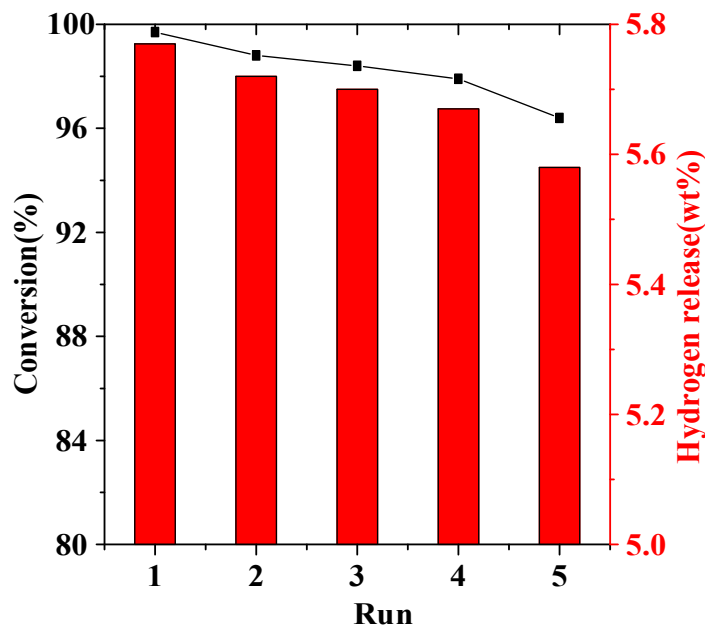


**Figure 7.** Conversion and hydrogen release of the 3.0 wt% Pd/CNTs in successive runs for the dehydrogenation of dodecahydro-N-ethylcarbazole at 533 K.

### 3. Materials and Methods

#### 3.1. Materials

All of the chemicals, such as N-ethylcarbazole (purity  $\geq 99.5\%$ , Shanghai Infine Chemicals Co., Ltd., Shanghai, China), ultra-high purity hydrogen (99.99999%, Minxing gas company), 5 wt.% Ru/Al<sub>2</sub>O<sub>3</sub> (reduced, Alfa aersa), C<sub>2</sub>H<sub>5</sub>OH (AR, Sinopharm Chemical Reagent Co., Ltd., Shanghai, China), Poly (N-vinyl-2-pyrrolidone) (PVP, Sinopharm Chemical Reagent Co., Ltd.), Palladium (II) chloride (AR, Nanjing Chemical Reagent Co., Ltd., Nanjing, China) and carbon nanotubes (CNTs,  $\Phi$  20–40 nm, Purity > 97%, Shenzhen Nanotech Port Co., Shenzhen, China), were utilized as purchased without further purification.

#### 3.2. Catalyst Preparation

CNTs were pretreated in a mixture of H<sub>2</sub>SO<sub>4</sub> (90 mL) and HNO<sub>3</sub> (60 mL) at 120 °C for 12 h. The treated CNTs were obtained by filtration, washing several times, and vacuum drying at 140 °C for 8 h.

A series of Pd-based catalysts were synthesized through immobilizing the ethanol reduction Pd nanoparticles (Pd NPs) onto the CNTs. In a typical synthesis, PdCl<sub>2</sub> was dissolved in an HCl aqueous solution to form an H<sub>2</sub>PdCl<sub>4</sub> aqueous solution. Then, PVP (0.4 g), H<sub>2</sub>O (40 mL), H<sub>2</sub>PdCl<sub>4</sub> aqueous solution (45 mL) and ethanol (60 mL) were refluxed at 90 °C for 3 h. The foregoing solution was treated through vacuum rotary evaporation and re-dispersed in ethanol to obtain the poly(N-vinyl-2-pyrrolidone)-stabilized Pd nanoparticles (PVP-Pd NPs) solution. Next, an appropriate amount of treated CNTs was added into the above-mentioned PVP-Pd solution under stirring. After another 3 h, the products were stirred to remove the excess solvent in the water bath. The obtained catalyst was dried at 70 °C for 4 h in a vacuum oven and then the X wt% Pd/CNTs catalysts were acquired after calcining at 550 °C for 3 h under a nitrogen atmosphere (X was the nominal Pd loading).

### 3.3. Hydrogen Generation from Dodecahydro-N-ethylcarbazole

Dodecahydro-N-ethylcarbazole was synthesized via the hydrogenation process using 5 wt% as catalysts for the dehydrogenation of N-ethylcarbazole. The detailed synthesis process has been previously reported [50].

The dehydrogenation of dodecahydro-N-ethylcarbazole was performed in a 25 mL round-bottomed flask in the presence of Pd/CNTs at a temperature ranging from 453 to 533 K. Specifically, 25 mg Pd/CNTs was placed in the round-bottomed flask, which was heated the desired temperature. Then, 5 mL of dodecahydro-N-ethylcarbazole was injected into the reactor under stirring. The evolved gas was measured by recording the displacement of water.

Durability for the catalysts. For testing the recyclability of the Pd/CNTs, after completing the dehydrogenation reaction, Pd/CNTs were separated from the reaction solution through centrifugation and washed with ethanol and water several times. The recovered Pd/CNTs were dried for the next experiment. The dehydrogenation reaction was repeated five times at the designed temperature.

### 3.4. Characterization

Powder X-ray diffraction (PXRD) patterns were obtained on a Bruker D8-Advance X-ray diffractometer using a Cu K $\alpha$  radiation source. X-ray photoelectron spectroscopy (XPS) was carried out using an Escalab 250Xi spectrometer with an Al K $\alpha$  source. BET surface areas were collected from N<sub>2</sub> adsorption/desorption isotherms at 77 K using automatic volumetric adsorption equipment (Micromeritics ASAP2020) after pretreatment under vacuum at 200 °C for 5 h. Transmission electron microscope (TEM) images were recorded on an FEI Tecnai F20 transmission electron microscope with an operating voltage of 200 kV. The metal content of the materials was collected on an inductively coupled plasma-atomic emission spectrometer (ICP-AES, Thermo iCAP6300). The exit gas composition was monitored using a Hiden QIC-20 quadruple mass spectrometer. Liquid samples were analyzed using a Shimadzu QP-2010S GC/MS with a Restek RTX5 30 m 0.25 mm capillary column according to the temperature program (100 °C isotherm for 2 min, then heated to 260 °C with a ramping rate of 10 °C/min).

## 4. Conclusions

In summary, we have developed an alcohol reduction method for the fabrication of Pd/CNTs with different palladium loadings. The as-synthesized 3.0 wt% Pd/CNTs exhibited outstanding catalytic performance for hydrogen release of dodecahydro-N-ethylcarbazole at 533 K with a conversion rate of 99.7% and 5.8 wt% H<sub>2</sub>. Furthermore, the activation energy for producing hydrogen from dodecahydro-N-ethylcarbazole catalyzed by 3.0 wt% Pd/CNTs was found to be  $43.8 \pm 0.2$  kJ mol<sup>-1</sup>. More importantly, the as-synthesized 3.0 wt% Pd/CNTs possess excellent cycle stability for the dehydrogenation of dodecahydro-N-ethylcarbazole. The reusability tests revealed that 3.0 wt% Pd/CNTs exhibited superior activity even five runs into the hydrogen evolution of dodecahydro-N-ethylcarbazole providing 96.4% conversion and 5.6 wt% H<sub>2</sub> at the fifth run. In addition, this simple synthesis means may provide a new avenue for the noble-metal and CNTs in dehydrogenation reaction.

**Supplementary Materials:** The following are available online at <http://www.mdpi.com/2073-4344/8/12/638/s1>, Figure S1: XRD patterns for the synthesized Pd/CNTs with 20 wt% Pd loading, Figure S2: Nitrogen adsorption-desorption isotherms for CNTs and 3.0 wt% Pd/CNTs, Figure S3: Pore size distribution for CNTs and 3.0 wt% Pd/CNTs, Table S1. The content of Pd in Pd/CNTs with different loading based on ICP-AES analysis.

**Author Contributions:** C.W., Y.A. and L.X. conceived and designed the experiments; M.Z. and M.Y. conducted the experiments, analyzed the data and wrote the manuscript; L.D. analyzed the physicochemical data.

**Funding:** This research was funded by the National Natural Science Foundation of China.

**Acknowledgments:** The authors acknowledge Anhui Provincial Natural Science Foundation (1608085QF156), Open Fund of Shaanxi Key Laboratory of Energy Chemical Process Intensification (SXECP1201601), Research Fund for Young Teachers of Anhui University of Technology (QZ201610), the National Natural Science Foundation of China (21376005), and the Scientific Research Foundation of Graduate School of Anhui University of Technology (2016012, 2016017, 2017082, 2017083).

**Conflicts of Interest:** The authors declare no conflicts of interest.

## References

1. Turner, J.A. Sustainable Hydrogen Production. *Science* **2004**, *305*, 972–974. [[CrossRef](#)] [[PubMed](#)]
2. Li, G.; Kanezashi, M.; Tsuru, T. Catalytic Ammonia Decomposition over High-Performance Ru/Graphene Nanocomposites for Efficient CO<sub>x</sub>-Free Hydrogen Production. *Catalysts* **2017**, *7*, 23. [[CrossRef](#)]
3. Li, J.; Li, B.; Shao, H.; Li, W.; Lin, H. Catalysis and Downsizing in Mg-Based Hydrogen Storage Materials. *Catalysts* **2018**, *8*, 89. [[CrossRef](#)]
4. Patil, S.P.; Pande, J.V.; Biniwale, R.B. Non-noble Ni–Cu/ACC bimetallic catalyst for dehydrogenation of liquid organic hydrides for hydrogen storage. *Int. J. Hydrogen Energy* **2013**, *38*, 15233–15241. [[CrossRef](#)]
5. Xu, L.X.; Liu, N.; Hong, B.; Cui, P.; Cheng, D.G.; Chen, F.Q.; An, Y.; Wan, C. Nickel–platinum nanoparticles immobilized on graphitic carbon nitride as highly efficient catalyst for hydrogen release from hydrous hydrazine. *RSC Adv.* **2016**, *6*, 31687–31691. [[CrossRef](#)]
6. Schlapbach, L.; Züttel, A. Hydrogen-storage materials for mobile applications. *Nature* **2001**, *414*, 353–358. [[CrossRef](#)] [[PubMed](#)]
7. Niaz, S.; Manzoor, T.; Pandith, A.H. Hydrogen storage: Materials, methods and perspectives. *Renew. Sustain. Energy Rev.* **2015**, *50*, 457–469. [[CrossRef](#)]
8. Zhu, Q.L.; Xu, Q. Liquid organic and inorganic chemical hydrides for high-capacity hydrogen storage. *Energy Environ. Sci.* **2015**, *8*, 478–512. [[CrossRef](#)]
9. Yao, F.; Li, X.; Wan, C.; Xu, L.X.; An, Y.; Ye, M.F.; Lei, Z. Highly efficient hydrogen release from formic acid using a graphitic carbon nitride-supported AgPd nanoparticle catalyst. *Appl. Surf. Sci.* **2017**, *426*, 605–611. [[CrossRef](#)]
10. Xia, Z.J.; Liu, H.Y.; Lu, H.F.; Zhang, Z.K.; Chen, Y.F. Study on catalytic properties and carbon deposition of Ni–Cu/SBA-15 for cyclohexane dehydrogenation. *Appl. Surf. Sci.* **2017**, *422*, 905–912. [[CrossRef](#)]
11. Bandaru, S.; English, N.J.; Phillips, A.D.; MacElroy, J.M.D. Exploring Promising Catalysts for Chemical Hydrogen Storage in Ammonia Borane: A Density Functional Theory Study. *Catalysts* **2017**, *7*, 140. [[CrossRef](#)]
12. Teichmann, D.; Arlt, W.; Wasserscheid, P.; Freymann, R. A future energy supply based on Liquid Organic Hydrogen Carriers (LOHC). *Energy Environ. Sci.* **2011**, *4*, 2767–2773. [[CrossRef](#)]
13. Jiang, Z.; Pan, Q.; Xu, J.; Fang, T. Current situation and prospect of hydrogen storage technology with new organic liquid. *Int. J. Hydrogen Energy* **2014**, *39*, 17442–17451. [[CrossRef](#)]
14. Markiewicz, M.; Zhang, Y.Q.; Bösmann, A.; Brückner, N.; Thöming, J.; Wasserscheid, P.; Stolte, S. Environmental and health impact assessment of Liquid Organic Hydrogen Carrier (LOHC) systems—challenges and preliminary results. *Energy Environ. Sci.* **2015**, *8*, 1035–1045. [[CrossRef](#)]
15. Patil, S.P.; Bindwal, A.B.; Pakade, Y.B.; Biniwale, R.B. On H<sub>2</sub> supply through liquid organic hydrides—Effect of functional groups. *Int. J. Hydrogen Energy* **2017**, *42*, 16214–16224. [[CrossRef](#)]
16. Teichmann, D.; Stark, K.; Müller, K.; Zöttl, G.; Wasserscheid, P.; Arlt, W. Energy storage in residential and commercial buildings via Liquid Organic Hydrogen Carriers (LOHC). *Energy Environ. Sci.* **2012**, *5*, 9044–9054. [[CrossRef](#)]
17. Wan, C.; An, Y.; Chen, F.Q.; Cheng, D.G.; Wu, F.Y.; Xu, G.H. Kinetics of N-ethylcarbazole hydrogenation over a supported Ru catalyst for hydrogen storage. *Int. J. Hydrogen Energy* **2013**, *38*, 7065–7069. [[CrossRef](#)]
18. Eblagon, K.M.; Tam, K.; Yu, K.M.K.; Zhao, S.L.; Gong, X.Q.; He, H.Y.; Ye, L.; Wang, L.C.; Ramirez-Cuesta, A.J.; Tsang, S.C. Study of Catalytic Sites on Ruthenium for Hydrogenation of N-ethylcarbazole: Implications of Hydrogen Storage via Reversible Catalytic Hydrogenation. *J. Phys. Chem. C* **2010**, *114*, 9720–9730. [[CrossRef](#)]
19. Preuster, P.; Papp, C.; Wasserscheid, P. Liquid Organic Hydrogen Carriers (LOHCs): Toward a Hydrogen-free Hydrogen Economy. *Acc. Chem. Res.* **2017**, *50*, 74–85. [[CrossRef](#)]
20. Sotoodeh, F.; Huber, B.J.M.; Smith, K.J. The effect of the N atom on the dehydrogenation of heterocycles used for hydrogen storage. *Appl. Catal. A* **2012**, *419–420*, 67–72. [[CrossRef](#)]

21. Crabtree, R.H. Nitrogen-Containing Liquid Organic Hydrogen Carriers: Progress and Prospects. *ACS Sustain. Chem. Eng.* **2017**, *5*, 4491–4498. [[CrossRef](#)]
22. Stark, K.; Emel'yanenko, V.N.; Zhabina, A.A.; Varfolomeev, M.A.; Verevkin, S.P.; Müller, K.; Arlt, W. Liquid Organic Hydrogen Carriers: Thermophysical and Thermochemical Studies of Carbazole Partly and Fully Hydrogenated Derivatives. *Ind. Eng. Chem. Res.* **2015**, *54*, 7953–7966. [[CrossRef](#)]
23. Papp, C.; Wasserscheid, P.; Libuda, J.; Steinrück, H.P. Liquid Organic Hydrogen Carriers: Surface Science Studies of Carbazole Derivatives. *Chem. Rec.* **2014**, *14*, 879–896. [[CrossRef](#)] [[PubMed](#)]
24. Arnende, M.; Gleichweit, C.; Werner, K.; Schernich, S.; Zhao, W.; Lorenz, M.P.A.; Hofert, O.; Papp, C.; Koch, M.; Wasserscheid, P. Model Catalytic Studies of Liquid Organic Hydrogen Carriers: Dehydrogenation and Decomposition Mechanisms of Dodecahydro-N-ethylcarbazole on Pt(111). *ACS Catal.* **2014**, *4*, 657–665.
25. Amende, M.; Schernich, S.; Sobota, M.; Nikiforidis, I.; Hieringer, W.; Assenbaum, D.; Gleichweit, C.; Drescher, H.J.; Papp, C.; Steinruck, H.P. Dehydrogenation Mechanism of Liquid Organic Hydrogen Carriers: Dodecahydro-N-ethylcarbazole on Pd(111). *Chem. Eur. J.* **2013**, *19*, 10854–10865. [[CrossRef](#)] [[PubMed](#)]
26. Gleichweit, C.; Amende, M.; Schernich, S.; Zhao, W.; Lorenz, M.P.A.; Hofert, O.; Bruckner, N.; Wasserscheid, P.; Libuda, J.; Steinruck, H.P. Dehydrogenation of Dodecahydro-N-ethylcarbazole on Pt(111). *ChemSusChem* **2013**, *6*, 974–977. [[CrossRef](#)] [[PubMed](#)]
27. Amende, M.; Gleichweit, C.; Schernich, S.; Höfert, O.; Lorenz, M.P.A.; Zhao, W.; Koch, M.; Obesser, K.; Papp, C.; Wasserscheid, P.; et al. Size and Structure Effects Controlling the Stability of the Liquid Organic Hydrogen Carrier Dodecahydro-N-ethylcarbazole during Dehydrogenation over Pt Model Catalysts. *J. Phys. Chem. Lett.* **2014**, *5*, 1498–1504. [[CrossRef](#)]
28. Sobota, M.; Nikiforidis, I.; Amende, M.; Zanon, B.S.; Staudt, T.; Hofert, O.; Lykhach, Y.; Papp, C.; Hieringer, W.; Laurin, M. Dehydrogenation of Dodecahydro-N-ethylcarbazole on Pd/Al<sub>2</sub>O<sub>3</sub> Model Catalysts. *Chem. Eur. J.* **2011**, *17*, 11542–11552. [[CrossRef](#)]
29. Peters, W.; Eypasch, M.; Frank, T.; Schwerdtfeger, J.; Korner, C.; Bosmann, A.; Wasserscheid, P. Efficient hydrogen release from perhydro-N-ethylcarbazole using catalyst-coated metallic structures produced by selective electron beam melting. *Energy Environ. Sci.* **2015**, *8*, 641–649. [[CrossRef](#)]
30. Peters, W.; Seidel, A.; Herzog, S.; Bosmann, A.; Schwieger, W.; Wasserscheid, P. Macrokinetic effects in perhydro-N-ethylcarbazole dehydrogenation and H<sub>2</sub> productivity optimization by using egg-shell catalysts. *Energy Environ. Sci.* **2015**, *8*, 3013–3021. [[CrossRef](#)]
31. Tarasov, A.L.; Tkachenko, O.P.; Kustov, L.M. Mono and Bimetallic Pt-(M)/Al<sub>2</sub>O<sub>3</sub> Catalysts for Dehydrogenation of Perhydro-N-ethylcarbazole as the Second Stage of Hydrogen Storage. *Catal. Lett.* **2018**, *148*, 1472–1477. [[CrossRef](#)]
32. Fei, S.X.; Han, B.; Li, L.L.; Mei, P.; Zhu, T.; Yang, M.; Cheng, H.S. A study on the catalytic hydrogenation of N-ethylcarbazole on the mesoporous Pd/MoO<sub>3</sub> catalyst. *Int. J. Hydrogen Energy* **2017**, *42*, 25942–25950. [[CrossRef](#)]
33. Sotoodeh, F.; Smith, K.J. Structure sensitivity of dodecahydro-N-ethylcarbazole dehydrogenation over Pd catalysts. *J. Catal.* **2011**, *279*, 36–47. [[CrossRef](#)]
34. Wang, Z.H.; Tonks, I.; Belli, J.; Jensen, C.M. Dehydrogenation of N-ethyl perhydrocarbazole catalyzed by PCP pincer iridium complexes: Evaluation of a homogenous hydrogen storage system. *J. Organomet. Chem.* **2009**, *694*, 2854–2857. [[CrossRef](#)]
35. Dong, Y.; Yang, M.; Mei, P.; Li, C.G.; Li, L.L. Dehydrogenation kinetics study of perhydro-N-ethylcarbazole over a supported Pd catalyst for hydrogen storage application. *Int. J. Hydrogen Energy* **2016**, *41*, 8498–8505. [[CrossRef](#)]
36. Yang, M.; Dong, Y.; Fei, S.X.; Ke, H.Z.; Cheng, H.S. A comparative study of catalytic dehydrogenation of perhydro-N-ethylcarbazole over noble metal catalysts. *Int. J. Hydrogen Energy* **2014**, *39*, 18976–18983. [[CrossRef](#)]
37. Kustov, L.M.; Tarasov, A.L.; Kirichenko, O.A. Microwave-activated dehydrogenation of perhydro-N-ethylcarbazole over bimetallic Pd-M/TiO<sub>2</sub> catalysts as the second stage of hydrogen storage in liquid substrates. *Int. J. Hydrogen Energy* **2017**, *42*, 26723–26729. [[CrossRef](#)]
38. Wang, B.; Chang, T.Y.; Jiang, Z.; Wei, J.J.; Zhang, Y.H.; Yang, S.; Fang, T. Catalytic dehydrogenation study of dodecahydro-N-ethylcarbazole by noble metal supported on reduced graphene oxide. *Int. J. Hydrogen Energy* **2018**, *43*, 7317–7325. [[CrossRef](#)]

39. Yazdan-Abad, M.Z.; Noroozifar, M.; Alfi, N.; Modarresi-Alam, A.R.; Saravani, H. A simple and fast method for the preparation of super active Pd/CNTs catalyst toward ethanol electrooxidation. *Int. J. Hydrogen Energy* **2018**, *43*, 12103–12109. [[CrossRef](#)]
40. Zhang, J.; Lu, S.F.; Xiang, Y.; Shen, P.K.; Liu, J.; Jiang, S.P. Carbon-Nanotubes-Supported Pd Nanoparticles for Alcohol Oxidations in Fuel Cells: Effect of Number of Nanotube Walls on Activity. *ChemSusChem* **2015**, *8*, 2956–2966. [[CrossRef](#)]
41. Xia, Y.; Ye, J.R.; Cheng, D.G.; Chen, F.Q.; Zhan, X.L. Identification of a flattened Pd–Ce oxide cluster as a highly efficient catalyst for low-temperature CO oxidation. *Catal. Sci. Technol.* **2018**, *8*, 5137–5147. [[CrossRef](#)]
42. Wang, B.; Yan, T.; Chang, T.Y.; Wei, J.J.; Zhou, Q.; Yang, S.; Fang, T. Palladium supported on reduced graphene oxide as a high-performance catalyst for the dehydrogenation of dodecahydro-N-ethylcarbazole. *Carbon* **2017**, *122*, 9–18. [[CrossRef](#)]
43. Wang, A.Q.; Li, J.; Zhang, T. Heterogeneous single-atom catalysis. *Nat. Rev. Chem.* **2018**, *2*, 65–81. [[CrossRef](#)]
44. Passaponti, M.; Savastano, M.; Clares, M.P.; Inclán, M.; Lavacchi, A.; Bianchi, A.; García-España, E.; Innocenti, M. MWCNTs-Supported Pd(II) Complexes with High Catalytic Efficiency in Oxygen Reduction Reaction in Alkaline Media. *Inorg. Chem.* **2018**, *57*, 14484–14488. [[CrossRef](#)] [[PubMed](#)]
45. Teranishi, T.; Miyake, M. Size Control of Palladium Nanoparticles and Their Crystal Structures. *Chem. Mater.* **1998**, *10*, 594–600. [[CrossRef](#)]
46. Wu, J.M.; Zeng, L.; Cheng, D.G.; Chen, F.Q.; Zhan, X.L.; Gong, J.L. Synthesis of Pd nanoparticles supported on CeO<sub>2</sub> nanotubes for CO oxidation at low temperatures. *Chin. J. Catal.* **2016**, *37*, 83–90. [[CrossRef](#)]
47. Koh, K.; Seo, J.-E.; Lee, J.H.; Goswami, A.; Yoon de, C.W.; Asefa, T. Ultrasmall palladium nanoparticles supported on amine-functionalized SBA-15 efficiently catalyze hydrogen evolution from formic acid. *J. Mater. Chem. A* **2014**, *2*, 20444–20449. [[CrossRef](#)]
48. Sotoodeh, F.; Huber, B.J.M.; Smith, K.J. Dehydrogenation kinetics and catalysis of organic heteroaromatics for hydrogen storage. *Int. J. Hydrogen Energy* **2012**, *37*, 2715–2722. [[CrossRef](#)]
49. Sotoodeh, F.; Zhao, L.; Smith, K.J. Kinetics of H<sub>2</sub> recovery from dodecahydro-N-ethylcarbazole over a supported Pd catalyst. *Appl. Catal. A Gen.* **2009**, *362*, 155–162. [[CrossRef](#)]
50. Wan, C.; An, Y.; Xu, G.; Kong, W. Study of catalytic hydrogenation of N-ethylcarbazole over ruthenium catalyst. *Int. J. Hydrogen Energy* **2012**, *37*, 13092–13096. [[CrossRef](#)]



© 2018 by the authors. Licensee MDPI, Basel, Switzerland. This article is an open access article distributed under the terms and conditions of the Creative Commons Attribution (CC BY) license (<http://creativecommons.org/licenses/by/4.0/>).